

Received March 15, 2022, accepted April 2, 2022, date of publication April 11, 2022, date of current version April 18, 2022.

Digital Object Identifier 10.1109/ACCESS.2022.3166632

Energy Efficient Local Path Planning Algorithm Based on Predictive Artificial Potential Field

RAFAL SZCZEPANSKI¹, (Member, IEEE), TOMASZ TARCZEWSKI¹, (Member, IEEE),
AND KRYSZTOF ERWINSKI¹, (Member, IEEE)

Faculty of Physics, Astronomy and Informatics, Institute of Engineering and Technology, Nicolaus Copernicus University in Torun, 87-100 Torun, Poland

Corresponding author: Rafal Szczepanski (szczepi@umk.pl)

This work was supported by the “Excellence Initiative - Research University” Programme of Nicolaus Copernicus University, Poland.

ABSTRACT Energy efficiency is one of the most important parameters in transportation electrification. It allows to improve the production rate due to longer operation without charging or decrease the cost related to transportation. To provide collision-free operation in unknown or various environment, the local path planning algorithm should be considered. An Artificial Potential Field (APF) algorithm is commonly used for this task, however it provides unsmooth and oscillating motion of autonomous ground vehicle (AGV), and is prone to being trapped in a local minimum, e.g. dead-end. In such a case, the energy used to achieve the goal position is higher than necessary. In this paper, the energy-efficient local path planning algorithm is proposed. Future movement prediction has been introduced to APF to allow AGV to bypass obstacles in advance. A novel method for local minimum avoidance is introduced. It is based on placement of virtual obstacles called *top quarks* in critical areas. These obstacles provide additional repulsive force for the APF based path planner. Considering the predicted stagnation-free path of the AGV, the new temporary goal for APF is selected. Such a combination allows to reduce traveled route length, improve its smoothness, and bypass local minima. The proposed Predictive Artificial Potential Field (PAPF) algorithm has been examined using Husarion ROSbot 2.0 PRO mobile robot, and the obtained results in form of videos are also attached as supplementary files. In comparison to original APF, the proposed path planning algorithm allows to reduce the used electric power by 21.4 %. PAPF provided a shorter path by up to 8.73 % and shorter time to reach the goal position by up to 40.23 %. The movement of the AGV is also much smoother in a case of usage of the proposed algorithm, and the proposed *top quarks*-based local minimum avoidance mechanism allows to bypass the local minima.

INDEX TERMS Artificial potential field, path planning, path prediction, autonomous ground vehicle, mobile robot.

I. INTRODUCTION

Nowadays, autonomous ground vehicles are gaining widespread adoption in industry (factories, warehouses) but also occur in every-day applications (e.g. self-driving cars [1], [2], restaurants [3], [4]). Main task of these vehicles is transportation of its load to goal position. In order to operate autonomously, the AGV requires implementation of path planning algorithm. This algorithm generates motion commands based on environment information provided by on-board sensors (local path planning algorithm) or information about the entire environment provided by an external source e.g. a predetermined static map (global path planning algorithm) [5]. In a dynamic environment, using

a global path planning algorithm may result in a potential collision because the algorithm does not take into account changes in the environment [6]. For this reason, usually the global path planner is used along with the local one, which is based on the AGV's perception and can provide collision-free path in dynamic environment, where the temporary obstacles occur [7]. Performance of the path planning algorithm is a key factor for increasing the production rate or shortening the production cycle. Multiple approaches to path planning optimality can be seen in the literature: minimum-time, minimum-jerk or minimum-energy [8]. In recent years, path planning algorithms have been intensively studied to improve the traveled path of AGV [9]. Global path planner, which generates entire path to the goal, can consider one of the above-mentioned optimality indicators, however the optimization in real-time is too complex and the robot needs

The associate editor coordinating the review of this manuscript and approving it for publication was Jie Gao¹.

some time to complete the calculations. For this reason, global optimization is done for a complex environment once, and then the pre-optimized trajectory is evaluated until the goal is reached [10]. For local path planner, the next position or linear velocity and direction of movement is calculated in real-time at every control loop period. For this reason, there is no simple way to define optimality criteria in overall traveled path by AGV.

The most popular path planning algorithms are: Dijkstra's algorithm, A-star algorithm, Probabilistic Roadmap algorithm, Rapidly-exploring random tree algorithm, and Artificial Potential Field algorithm. Dijkstra's algorithm searches for the shortest path between nodes in a graph [11]. In a case of the path planning problem, the connection cost is related to distance, and it can provide the shortest path to the goal [12]. The algorithm examines all neighbors of the parent node, and then it considers these neighbors as a next parent node. The graph is expanding to explore entire environment. To improve performance of the algorithm in the path planning problem, Dijkstra's algorithm has been modified by adding a priority queue in a case to examine the nodes which are closer to the goal. This modification is called A-star and nowadays is one of well-known path planning algorithms [13]. It allows to reduce the explored environment during the path planning process. Such a modification significantly reduces the computation time without any drawback on the algorithm's convergence. Probabilistic Roadmap and Rapidly-exploring random tree algorithms are the most popular sampling-based algorithms. The first one is based on randomly generating nodes of graph in free space and connecting them in line if such a connection is collision-free. Then Dijkstra's algorithm is used to find the connection between the AGV and the goal. The algorithm is repeated until there is no connection between these points [14]. Rapidly-exploring random tree algorithm is based on tree growing [15]. The algorithm starts with a random configuration and then it is expanding in the environment. The tree is growing until there is no connection the the goal. Another approach to solve the path planning problem is application of optimization algorithms. In the literature, multiple approaches with different algorithms, objectives and requirements have been evaluated, e.g., membrane evolutionary algorithm [16], [17], particle swarm optimization algorithm [18], [19], bat algorithm [20], ant colony algorithm [21], grey wolf optimization [22]. The common requirement of the above-mentioned approaches is to have complete knowledge about the environment in which the path of the AGV is planned. In many applications, such a requirement can be acceptable, but in general, the environment, e.g., warehouse or factory, may change due to unpredictable situations. Such an application requires local path planner based on on-line information obtained from on-board sensors.

The pioneering and most popular local path planning algorithm is the Artificial Potential Field algorithm proposed by Khatib in 1985 [23]. The APF algorithm navigates AGV

to the goal by continuous attractive and repulsive fields. The attractive one is related to the goal reaching task, while the repulsive fields are generated by obstacles. A combination of them allows the AGV to reach a goal and provide a collision-free movement in unknown environment. Unlike other methods, the APF calculates subsequent linear and angular velocities in real time considering only data obtained from on-board sensors. It does not require a map of the entire environment. Due to this advantage, it is commonly used in the path planners implemented in AGVs [24]. However, using the APF algorithm may result in the vehicle getting trapped at a local minimum [25]. Furthermore, measurement noise and imprecision in physical implementation may result in oscillations and generation of a non-smooth path [26]. To alleviate the disadvantages of APF, researchers have proposed multiple modifications of the original algorithm, but these modifications do not cover all mentioned aspects. In [27], the robot perception is extended by augmented reality technology to bypass the local minima. The virtual wall has been added to APF algorithm to prevent the mobile robot from falling in the local minimum. In addition, the direction of the robot's movement is forced by a virtual obstacle. The proposed algorithm allows to decrease the traveled path by the mobile robot in comparison to existing methods. Nevertheless, the smoothness of the movement has not been taken into account. The APF has been improved by a nature-inspired optimization algorithm by optimizing the APF parameters in collision avoidance in [28]. The presented approach allows to decrease the path length and ensures the collision-free movements of the SCARA robotic arm, but both problems related to movement smoothness and local minimum avoidance are not addressed simultaneously. A waypoint tracking scheme with a collision-avoidance system using the APF with speed planning is proposed in [29]. Since the local path planner does not usually conform to the dynamic constraints of the vehicle motion, the authors proposed a method to combine the dependence of the vehicle's speed with the curvature of the path. Such an approach allows to eliminate severe yawing of the heading angle of the vehicle, and it prevents possible excessive tire slip angle of the vehicle driving at high speed. The proposed approach is not applicable for environments with local minima due to lack of the avoidance mechanism. In [30], membrane pseudo-bacterial potential field algorithm has been proposed. The algorithm uses dynamic membranes that include a pseudo-bacterial genetic algorithm for evolving the required parameters of APF algorithm. The goal of the proposed algorithm was to minimize path length, ensure collision avoidance, and provide path smoothness. Obtained results indicate proper operation of the proposed solution, however the local minimum avoidance has not been considered. In [31], the integration of unmanned aircraft vehicles (UAVs) in the dynamic national airspace to prevent them from colliding with the other traffics. To solve the problem, the authors proposed the dynamic APF algorithm, which allows to generate a real-time reactive collision-free

path for unmanned aircraft vehicles flying in dynamic airspace. The proposed dynamic APF can prevent the UAV from colliding into nearby unexpected moving obstacles. This approach can be used to reduce the impact of UAVs on nearby users of the airspace. Although topic is interesting from the application point of view, the path smoothness and local minimum avoidance have not been solved. In [32] the improved black-hole potential field method and reinforcement learning are combined to avoid the local minima. Such a combination allows agents to automatically adapt to the environment with local minima. Agents can reach the goal in an environment with new types of obstacles and dynamic goal using the adaptation mechanism in real-time. The warehouse problem is considered, and the efficiency of the proposed method has been proved. Regardless of the proposed local minima avoidance mechanism, smoothness of movement has not been improved. In [33], a vehicle lane change system using model predictive path planning based on APF for speeding vehicles is proposed. It introduces a novel combination of APF algorithm with a curve-fitting method to consider vehicle dynamics for the lane-keeping system. The proposed algorithm uses a curve fitting method under vehicle dynamic constraints to plan a safe-feasible path based on calculated waypoints by APF algorithm. The simulation results proved that the model predictive path planning algorithm is highly effective in high-speed lane change scenarios to avoid dynamic obstacle vehicles. However, in a case of the local minimum occurrence, the algorithm can stagnate and it will not reach the goal. Prediction-based APF approach was presented in [34]. It is based on the subsequent obstacle detection, and then the final movement direction of the AGV is corrected to smooth the traveled path. The proposed algorithm modifies the direction of AGV, considering the extreme points of the object in front of the vehicle. It allows AGV to react in advance to the obstacle, but the examinations were provided only for a single obstacle environment. In a multi-obstacle environment, the perception of the AGV is limited, and in some situations, the extreme points of the object cannot be appointed. Moreover, in case of modification of the orientation obtained from the original APF, the collision-free cannot be guaranteed in a complex environment, i.e., the modified direction may generate a collision with another obstacle. In addition, the algorithm lacks a local minimum avoidance mechanism.

From the presented literature overview, one can see that the solution where all above-mentioned disadvantages are overcome does not exist. In a case of development of energy-efficient local path planning algorithm, all these aspects should be provided at once with collision-free operation. The authors' motivation of the novel APF modification was to provide:

- collision-free operation,
- relatively short path,
- smooth movement,
- local-minimum bypassing mechanism.

All the mentioned assumptions were made to increase the energetic-efficiency of the AGV. To the best of authors' knowledge, such complex requirements of local path planning approach have not been investigated yet.

In this paper, the APF is improved by application of the prediction of future movements. Such an approach allows to decrease the path length and also make a traveled path smoother. The proposed approach has a built-in a local minimum avoidance mechanism based on virtual objects. The proposed Predictive APF is based on selection of new temporary goal for original APF algorithm [23]. The temporary goal is selected to move in direction that is required to bypass the obstacle. For this reason, the obtained path is shorter and stagnation in local minimum does not occur. The experimental examinations have been made on Husarion ROSbot 2.0 PRO mobile robot with Robot Operating System. Furthermore a video presentation of the obtained results is attached in the supplementary files. In addition, the energetic efficiency has been evaluated to compare the original APF and the proposed PAPP.

The paper is organized as follows. Section II describes the original APF algorithm with marked implementation requirements. The proposed PAPP algorithm is presented in Section III, including precise description of the path prediction algorithm, and selection of new temporary goal procedure. In-depth analysis of the proposed PAPP algorithm performance and impact of its parameters on traveled path by AGV is presented in Section IV. Finally, Section V presents our conclusions.

II. ARTIFICIAL POTENTIAL FIELD ALGORITHM

The Artificial Potential Field algorithm proposed in 1985 is currently the state-of-the-art in local path planning [23]. It is based on the electrostatic particles interaction given by eq. (1) [35].

$$F = -\frac{kq_1q_2}{r^2} \quad (1)$$

where: k is the interactions constant; q_1 and q_2 are the electric charges of the particles; and r is the distance between the particles. The algorithm is divided into to potential forces: attractive (opposite particles' charges $q_1 = -q_2$) and repulsive (identical particles' charges $q_1 = q_2$). In order to provide the collision-free and goal reaching path, the obstacles and AGV are assumed as having the same charge and the goal position is opposite charge particle. In such a case, the obstacle generates repulsive force and the goal position generates attractive force. The graphical representation of the APF algorithm is presented in Fig. 1. The overall force that is applied to AGV is depicted in eq. (2).

$$\vec{F}_w = \vec{F}_{goal} + \vec{F}_{obstacles} \quad (2)$$

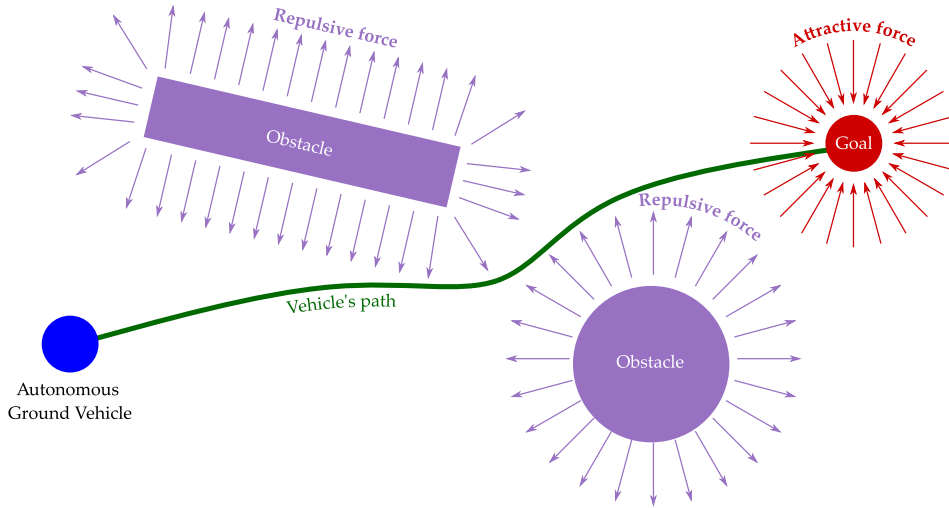


FIGURE 1. The graphical representation of the artificial potential field's forces.

with

$$\vec{F}_{goal} = -\frac{k_{VG}q_Vq_G}{|\vec{r}_{VG}|^2} \cdot \frac{\vec{r}_{VG}}{|\vec{r}_{VG}|}$$

$$\vec{F}_{obstacles} = -\sum_{i=1}^N \begin{cases} \frac{k_{VO}q_Vq_O}{|\vec{r}_{VO_i}|^2} \cdot \frac{\vec{r}_{VO_i}}{|\vec{r}_{VO_i}|}, & \text{if } |\vec{r}_{VO}| \leq d_o \\ 0, & \text{otherwise} \end{cases}$$

where \vec{F}_{goal} is the attractive force; $\vec{F}_{obstacles}$ is the repulsive force; k_{VG} and k_{VO} is the interaction constant between AGV and the goal, and the AGV and obstacles; q_V , q_G and q_O is the AGV, the goal, and obstacles charge, respectively; N is a number of obstacles in AGV's surroundings; \vec{r}_{VG} and \vec{r}_{VO_i} is the directional vector from the AGV to the goal and from the AGV to i -th obstacle; and d_o is a repulsive effective range.

From the obtained \vec{F}_w , the next direction and linear velocity of the AGV can be calculated using eq. (3)-(4).

$$\theta^* = \arctan\left(\frac{F_w^y}{F_w^x}\right) \tag{3}$$

where: θ^* is reference AGV's orientation.

$$V^* = \text{Limit}\left(|\vec{F}_w|, V_{max}\right) \tag{4}$$

where: V^* is reference AGV's linear velocity; and V_{max} is maximum allowed AGV's linear velocity. These equations work properly only in simulation case due to AGV limited dynamics. It is not possible to change the AGV orientation rapidly. For this reason, the AGV can go dangerously near the obstacle. To prevent this, the linear velocity equation should take into account the error (θ_{error}) between the reference orientation (θ^*) and current orientation (θ). The high error value has to decrease the linear velocity. The modified linear velocity equation is as follows:

$$V^* = \begin{cases} \text{Limit}\left(\alpha \cdot |\vec{F}_w|, V_{max}\right), & \text{if } \text{abs}(\theta_{error}) \leq \theta_{error}^{max} \\ 0, & \text{otherwise} \end{cases} \tag{5}$$

with:

$$\alpha = \frac{\theta_{error}^{max} - \text{abs}(\theta_{error})}{\theta_{error}^{max}}$$

where: θ_{error}^{max} is a margin orientation error. In this approach, linear velocity depends linearly on θ_{error} in range $\langle -\theta_{error}^{max}, \theta_{error}^{max} \rangle$ and is zero if the AGV's orientation error exceed the range.

Unfortunately, the algorithm has a few problems [25], which are illustrated in Fig. 2, and described below:

- a There is no mechanism of avoiding or bypassing the dead-ends. If a vehicle enters a dead-end, it cannot get out without human intervention or another mechanism.
- b In very narrow passages, the repulsive force generated by the walls can stop the robot from getting between them. In this situation, the goal will not be reached.
- c The algorithm generates an oscillation in the presence of obstacles, which is mainly related to the limited dynamics of the vehicle. The obtained orientation and linear velocity from the algorithm are set as reference values to the motion controller of the vehicle, and additional time is required to obtain proper orientation and speed.
- d The same situation occurs in narrow corridors. It should be noted that the oscillations can be unstable and eventually cause a collision.

A. ENERGETIC EFFICIENCY ANALYSIS

AGV's are usually battery powered so the evaluation of a path generation algorithm should also take into account the energy consumption aspect. It is often preferable to utilize a longer but smoother path which does not require sudden accelerations. Such rapid maneuvers increase current consumption and shorten the operation lifespan of the AGV. The total energy of the AGV can be expressed using the

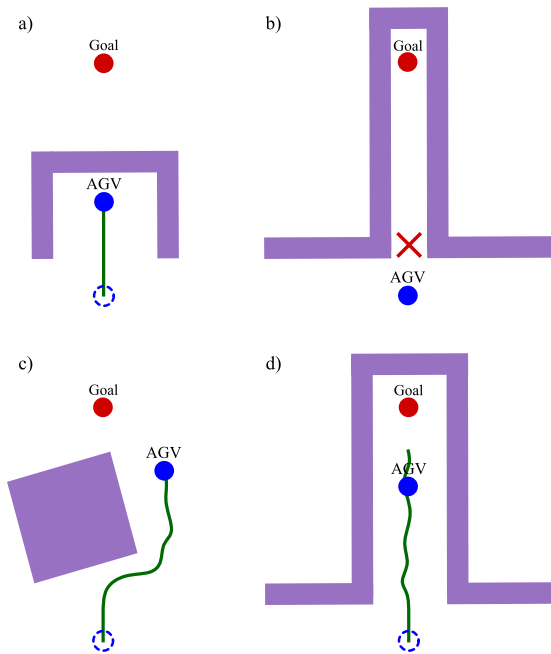


FIGURE 2. Problems with potential field methods.

following formula [36]:

$$E(t) = \int_t \left(mv(t)a(t) + I\omega(t)\beta(t) + \frac{2f_v}{r}v(t) + B \right) dt + P_s t \tag{6}$$

where: m is AGV mass; I is AGV moment of inertia; f_v is a viscous friction coefficient; B is fixed power provided for the motors to overcome the static friction; P_s is other energy consumed for on-board embedded computer, sensors, and control circuit; $v(t)$ and $a(t)$ are linear velocity and acceleration, respectively; $\omega(t)$ and $\beta(t)$ are angular velocity and acceleration, respectively; From the depicted equation, one can see that energy is complex function where linear and angular velocity and acceleration have an impact on its terminal value. For this reason, smoother path will decrease the energy consumption. Next, the integration in time domain causes that shorter time required to travel the route may also decrease the required energy to reach the goal. Due to lack of local minima avoidance mechanism in APF algorithm and its susceptibility to oscillations, the above analysis of eq. 6 undermines energetic efficiency of the original APF algorithm.

III. THE PROPOSED PREDICTIVE-APF

The keynote of the proposed PAPF algorithm is to obtain shorter and smoother path with a shorter time to reach the goal, and bypass the local minima in order to provide energy efficient path planning algorithm. To obtain such a behaviour of the path planning algorithm, the authors developed a prediction-based approach. In real-time, the future movements are predicted to obtain the next path in predetermined horizon of prediction. This information is used

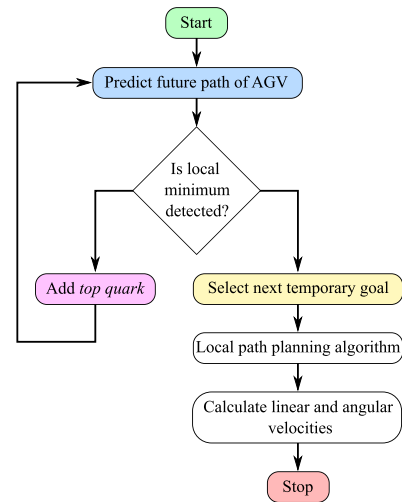


FIGURE 3. The general diagram of the proposed predictive artificial potential fields algorithm.

to determine the temporary goal for the AGV. Therefore, the current direction of AGV is corrected to react to obstacles in advance, and avoid unnecessary movements. In addition, the predicted path is used to detect AGV’s stagnation in the local minimum. In such a case, the virtual obstacles, called *top quarks*, are created to force the AGV to select goal-reaching path. The general diagram of the proposed Predictive Artificial Potential Fields algorithm is presented in Fig. 3

A. PREDICTION OF FUTURE MOVEMENTS

The visualization of the proposed prediction mechanism is presented in Fig. 4, while algorithms steps are enumerated below:

- (i) First a direction line is defined as current original APF force direction,
- (ii) Successive path positions are generated using the original APF algorithm with a constant position increment and predefined number of steps,
- (iii) Perpendicular distance between each point and the direction line is computed,
- (iv) The point with the largest distance is selected as the new temporary goal,
- (v) New APF force is calculated for the temporary goal instead of the global one for the AGV’s movement.

The prediction of future movements is based on the state-of-the-art local path planning algorithm, which is APF in this particular case. The novel algorithm uses only two intuitive parameters: horizon of prediction (λ) and step-size (Δ). The first one determines length of the predicted path, e.g., 2 m, while the second one is used to manipulate the distance between consecutive points, e.g., 0.01 m. The next position of AGV is generated using the original APF algorithm with constant position increment (Δ) until the final predicted trajectory path is shorter than the predefined horizon of prediction (λ). Using eq. (2) and eq. (3) for previous predicted position as actual one, the direction of next step is obtained.

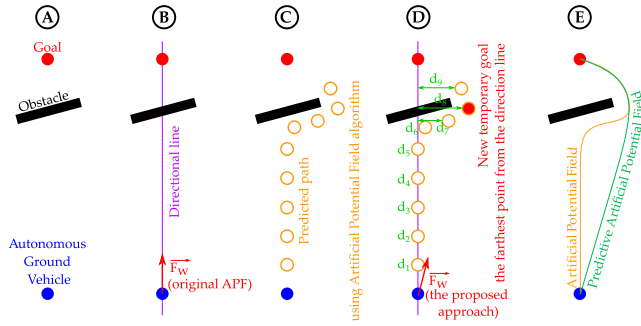


FIGURE 4. The idea of the proposed path planning algorithm based on the APF and path prediction.

Next the predicted position is updated in this direction by step-size. Such a prediction allows to obtain local path in predefined horizon, which will be used in the next steps of PAPP algorithm. The path prediction procedure is presented in Algorithm 1:

Algorithm 1 Path Prediction Algorithm

- 1: Set $predicted_path[0]$ to current AGV position
- 2: Set $goal$ to global goal position
- 3: Set i_{max} to λ/Δ
- 4: **for** $i = 1$ to i_{max} **do**
- 5: Calculate APF force \vec{F}_w for previous position ($predicted_path[i - 1]$)
- 6: Set $predicted_path[i]$ as $predicted_path[i - 1]$ moved in obtained direction by Δ
- 7: **end for**
- 8: return($predicted_path$)

It should be noted that the prediction is calculated in real-time on the AGV. For this reason, the step-size should be small enough to provide the highest accuracy of predicted path, and large enough to allow the real-time prediction, e.g., for above-mentioned parameters, the prediction requires to calculate the APF algorithm 200 times per control loop.

Next, the obtained predicted path is used to determine new temporary goal for AGV in order to provide shorter and smoother path.

B. TOP QUARK-BASED MECHANISM

One of the main problem of APF algorithm, and many other local path planning algorithms, is the stagnation in local minimum. To solve the problem, the additional mechanism is required [35]. In the proposed PAPP algorithm, the novel local minimum avoidance mechanism is based on detection of algorithm stagnation during the described prediction of future movements. In such a case, a virtual heavy particle, called *top quark* (which is the most massive of all observed elementary particles), is placed in the detected local minimum and then the prediction of future movements procedure is

repeated until the predicted path is free of the stagnation problem. In order to solve dead-lock related to the lack of non-stagnation path, the maximum number of repetition is limited to M times. The *top quark* has been called heavy due to significantly larger interaction constant (k_{VQ}) assumed for this kind of obstacle (i.e., $k_{VQ} \ll k_{VQ}$). The modified force equation including the proposed *top quarks* is as follows:

$$\vec{F}_w = \vec{F}_{goal} + \vec{F}_{obstacles} + \vec{F}_{top\ quark} \tag{7}$$

with

$$\vec{F}_{top\ quark} = - \sum_{i=1}^{M_{curr}} \begin{cases} \frac{k_{VQ}q_Vq_Q}{|\vec{r}_{VQ_i}|^2} \cdot \frac{\vec{r}_{VQ_i}}{|\vec{r}_{VQ_i}|}, & \text{if } |\vec{r}_{VQ}| \leq d_o \\ 0, & \text{otherwise} \end{cases}$$

where $\vec{F}_{topquark}$ is the repulsive force; k_{VQ} is the interaction constant between AGV and *top quarks*; q_Q is *top quark* charge; M_{curr} is a number of created *top quarks* by the proposed local minimum avoidance mechanism ($0 \leq M_{curr} \leq M$); \vec{r}_{VQ_i} is the directional vector from the AGV to i -th *top quark*; and d_o is a repulsive effective range. The idea of the novel *top quark* local minimum avoidance mechanism proposed in this paper and used in the PAPP algorithm is presented in Fig. 5. The figure presents the six iterations (subfigures B-G) of future path prediction. It is shown that each stagnation point in previous prediction is used to place the *top quark*. The next path prediction take into the account *top quark* in the same way as the other obstacles but with higher interaction constant (k_{VQ}).

The detection of the local minimum is based on a prediction of additional path-length ($\lambda_{stagnation}$) and calculating the the mean position of these predicted points ($\vec{p}_{stagnation}$). If all predicted points are in a range equal to R from the mean position then it is assumed that the robot's stagnation problem occurs. Next, the *top quark* is placed to $\vec{p}_{stagnation}$, and the procedure of prediction of future path is repeated. The result of the proposed local-minimum avoidance mechanism is stagnation-free path that is used to select new temporary goal.

C. SELECTION OF NEW TEMPORARY GOAL

The new temporary goal is selected as the most distant point from the last predicted path, i.e., stagnation-free path, from the direction of classic APF. The procedure of the selection is as follows:

- (i) calculate the \vec{F}_w force for current AGV's position,
- (ii) create a linear function (i.e., $A \cdot x + B \cdot y + C = 0$, where: x and y are the point coordinates; A , B and C are the function parameters) of the direction of obtained force called as directional line,
- (iii) calculate distance (d) between each position (\vec{p}) in the predicted path and the directional line using following formula:

$$d = \frac{|A \cdot p^x + B \cdot p^y + C|}{\sqrt{(A^2 + B^2)}} \tag{8}$$

- (iv) select the farthest point from the directional line.

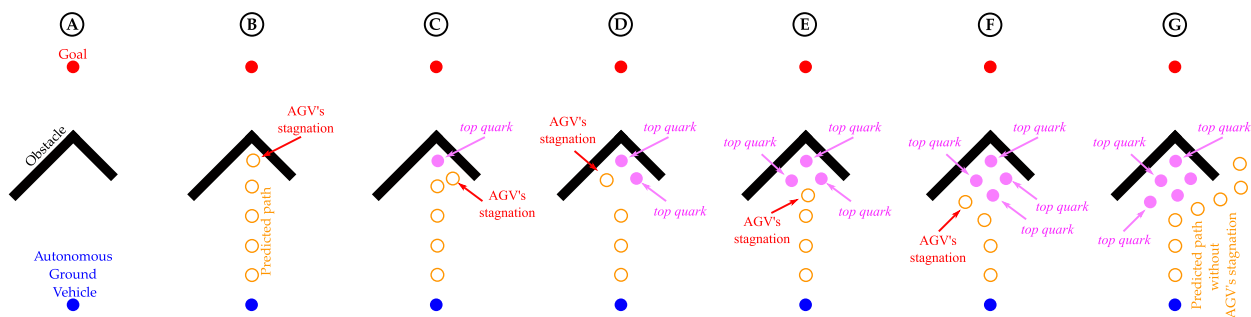


FIGURE 5. Top quark-based local minimum avoidance mechanism used in the proposed PAPF algorithm.

TABLE 1. Parameters of APF and PAPF algorithms.

Parameter	Value
Common parameters	
LiDAR data points (L)	300
q_V, q_O	-1
q_G	1
k_{VG}	5
k_{VO}	$10 \div L$
θ_{error}^{max}	30 deg
Goal position (x, y)	(2.2, 2.7) m
PAPF parameters	
λ	1.0 m
Δ	0.03 m
q_Q	-1
k_{VQ}	$5 \cdot k_{VO}$
$\lambda_{stagnation}$	$0.25 \cdot \lambda$ m
R	$0.25 \cdot \lambda_{stagnation}$ m
M	10

Such a definition of new temporary goal is supported by triangle inequality, which states that for any triangle, the sum of the lengths of any two sides must be greater than or equal to the length of the remaining side. If in the predicted path, the obstacle forced AGV to avoid it, then the most distant point from the initial direction is selected, so the AGV moves to this position in advance. The additional remark should be noted: when the obstacle is just in range of horizon of prediction, then the temporary goal will be moved smoothly from the direction path to goal, to the point that has to be reached to avoid the obstacle during next AGV positions. These two information proves that the obtained path by PAPF should be shorter and smoother (or at least the same) then the one obtained by APF.

D. CALCULATE NEXT AGV's LINEAR VELOCITY AND ORIENTATION

The last step in the proposed PAPF is to calculate the linear velocity and orientation of AGV. The PAPF uses the modified APF equation of \vec{F}_w force (eq. (7)), but it takes the temporary goal instead of the global one. Next, the linear velocity and orientation is calculated using eq. (3) and eq. (5).

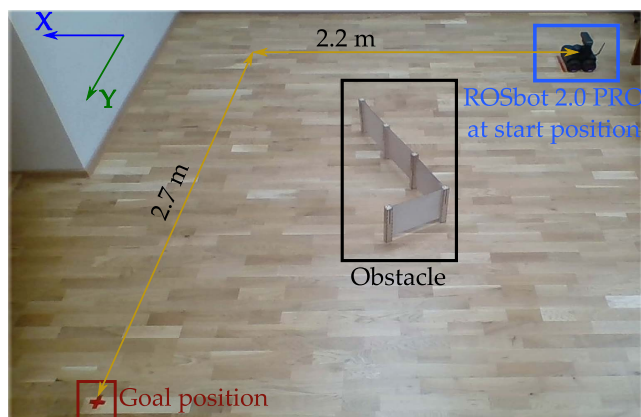


FIGURE 6. The photo of laboratory environment for test (I).

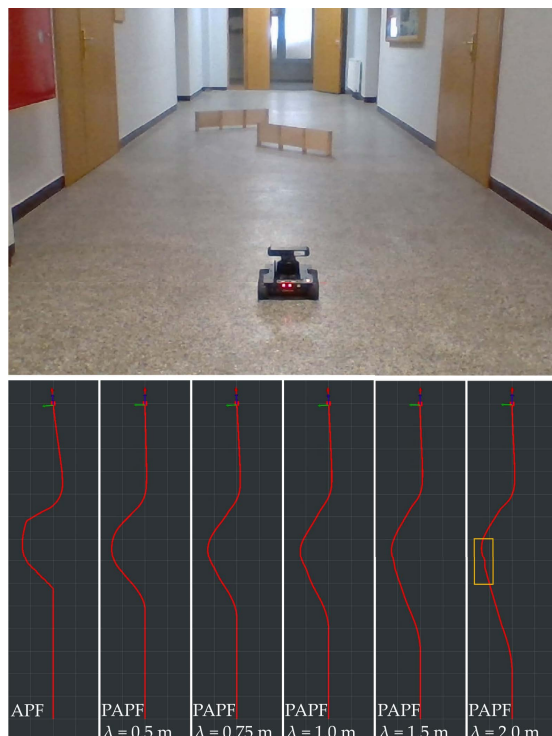


FIGURE 7. Impact of the horizon of prediction to shape of traveled path by AGV.

It is worth to point out that the proposed PAPF algorithm should guarantee collision-free path due to usage of the

TABLE 2. Indicators obtained in Test (I)-(V).

	Artificial Potential Field		Predictive Artificial Potential Field	
	Duration [s]	Path length [m]	Duration [s]	Path length [m]
Test (I)	69.79	4.50	41.71 (reduced by 40.23 %)	4.13 (reduced by 8.29 %)
Test (II)	52.12	4.20	41.366 (reduced by 20.63 %)	4.16 (reduced by 1.00 %)
Test (III)	42.22	3.99	37.89 (reduced by 10.45 %)	3.80 (reduced by 4.78 %)
Test (IV)	fail	fail	38.424	3.77
Test (V)	fail	fail	39.426	3.87
Test (VI)	49.15	4.05	41.93 (reduced by 14.69 %)	3.76 (reduced by 7.16 %)

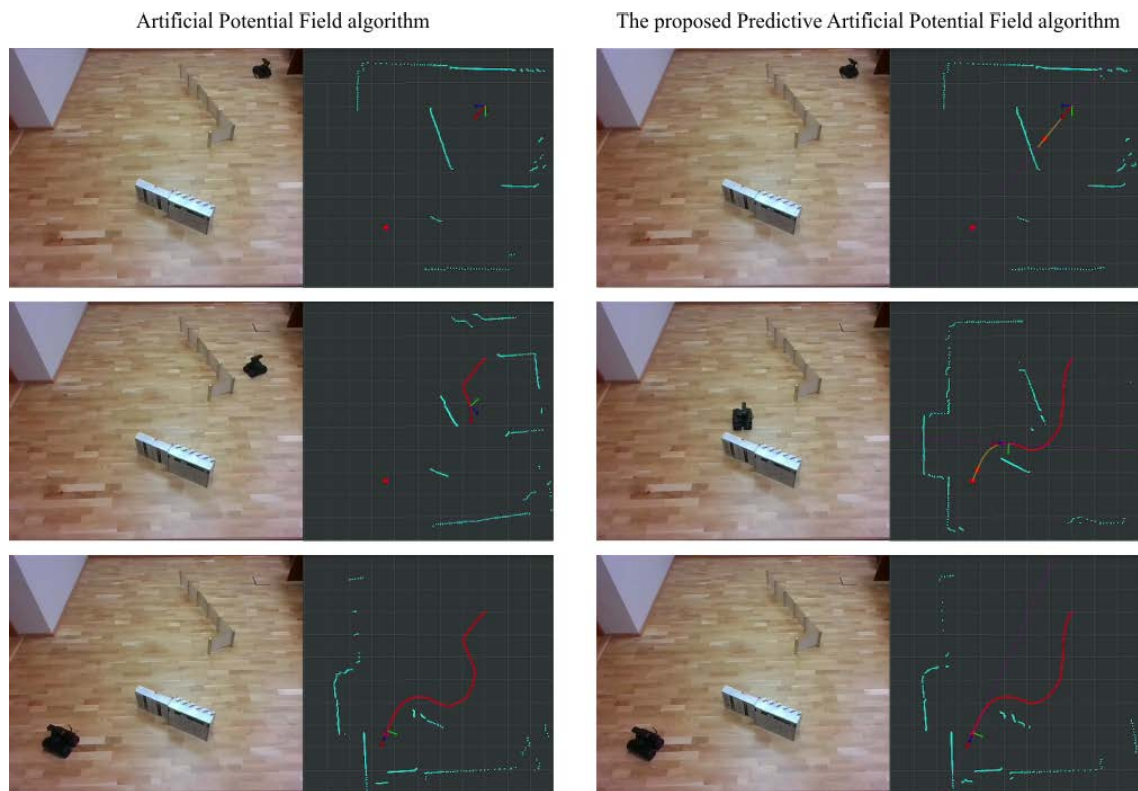


FIGURE 8. Comparison of the proposed PAPP and the classical APF algorithms in Test (I).

extended APF equations. Modifications of the original approach is generating temporary goal instead of calculated force for global goal, and in a case of local minimum occurrence, considering *top quarks*.

IV. EXPERIMENTAL VALIDATION

The validation of the proposed prediction-based path planning algorithm was made using the Husarion ROSbot 2.0 PRO mobile robot and Robot Operating System. The APF and PAPP algorithms were implemented in C++ programming language and they are based only on the LiDAR sensor (i.e., 360 degree laser scanner).

The photo of the laboratory environment is presented in Fig. 6, while the algorithms parameters are summarized in Table 1.

In a case of APF parameters, which are common for both algorithms, they have been chosen taking into account mobile robot size, the environment size, and obstacles size. In addition, the interaction constants were selected empirically to provide a collision-free movement with safe margin to obstacles. For the proposed PAPP algorithm, the horizon of prediction (λ) is the most important parameter and selection process has been visualized in next subsection. The step-size (Δ) and coefficients in the rest of parameters were selected empirically with particular emphasis on the correctness

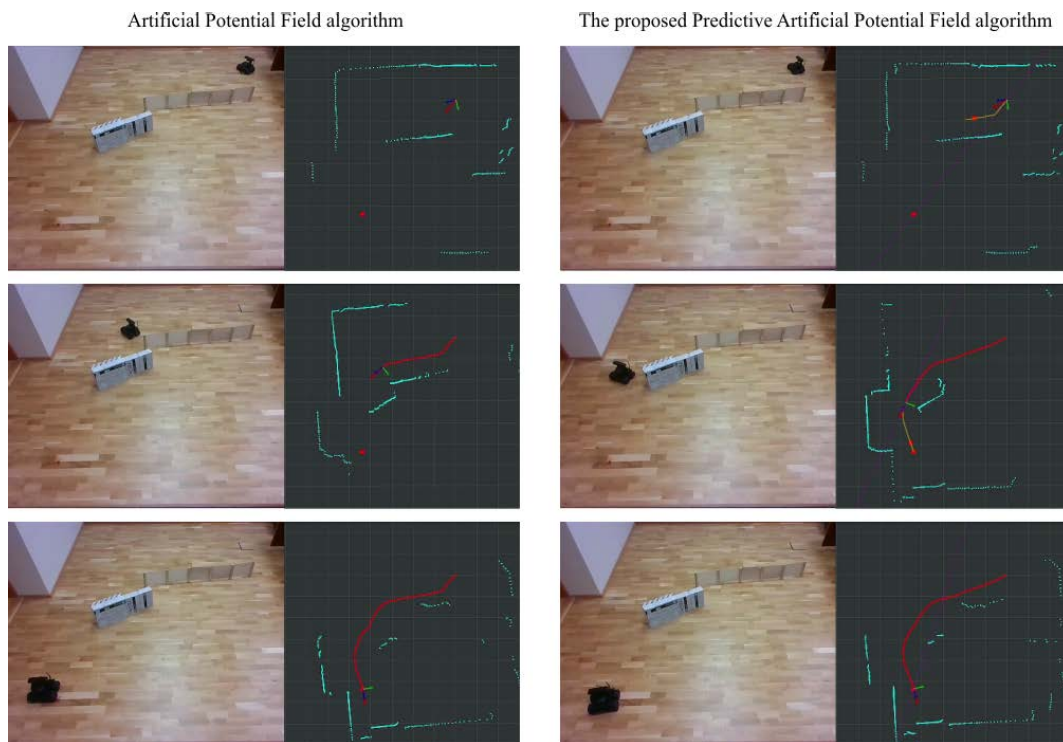


FIGURE 9. Comparison of the proposed PAPF and the classical APF algorithms in Test (II).

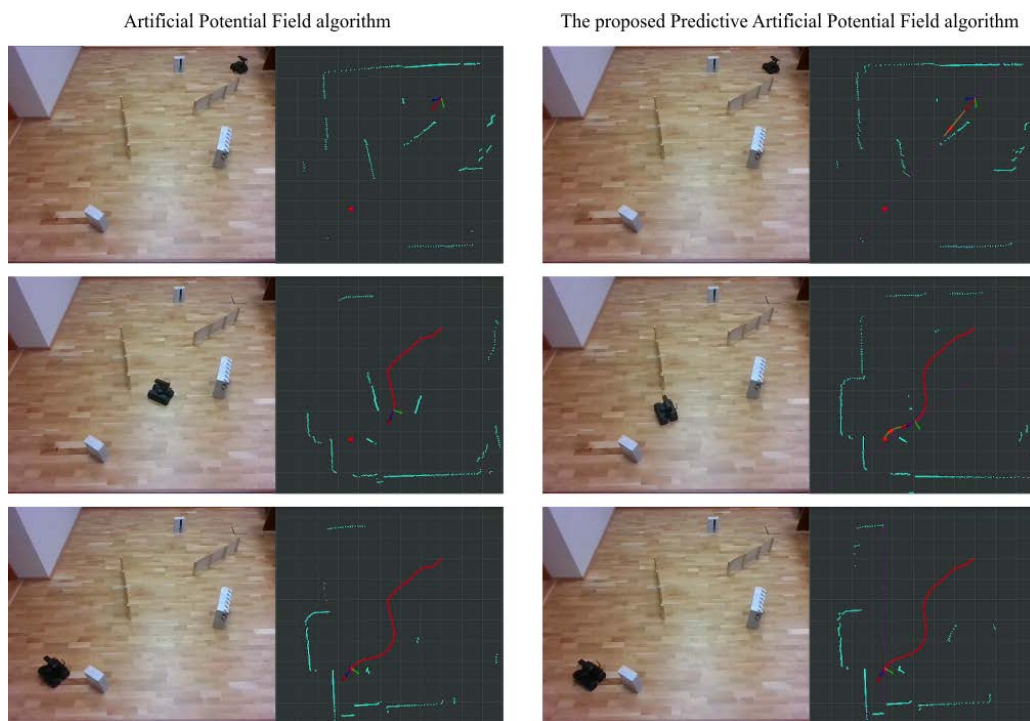


FIGURE 10. Comparison of the proposed PAPF and the classical APF algorithms in Test (III).

of stagnation detection and computational requirements of prediction. Calculation time of path prediction in ROSbot 2.0 PRO is as follows:

- $\lambda = 1$ m and $\Delta = 0.01$ m:
 - single path prediction takes 15 ms;
 - M paths prediction takes 147 ms
- $\lambda = 1$ m and $\Delta = 0.03$ m:
 - single path prediction takes 5 ms;
 - M paths prediction takes 51 ms
- $\lambda = 2$ m and $\Delta = 0.03$ m:
 - single path prediction takes 10 ms;
 - M paths prediction takes 98 ms

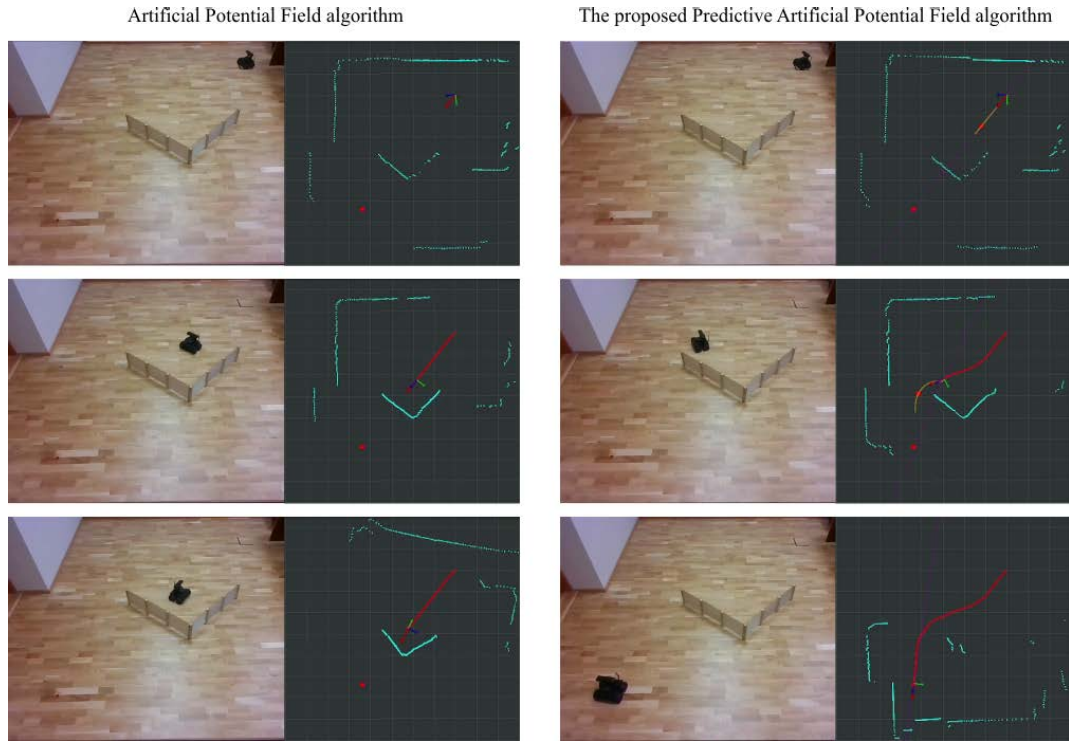


FIGURE 11. Comparison of the proposed PAPF and the classical APF algorithms in Test (IV).

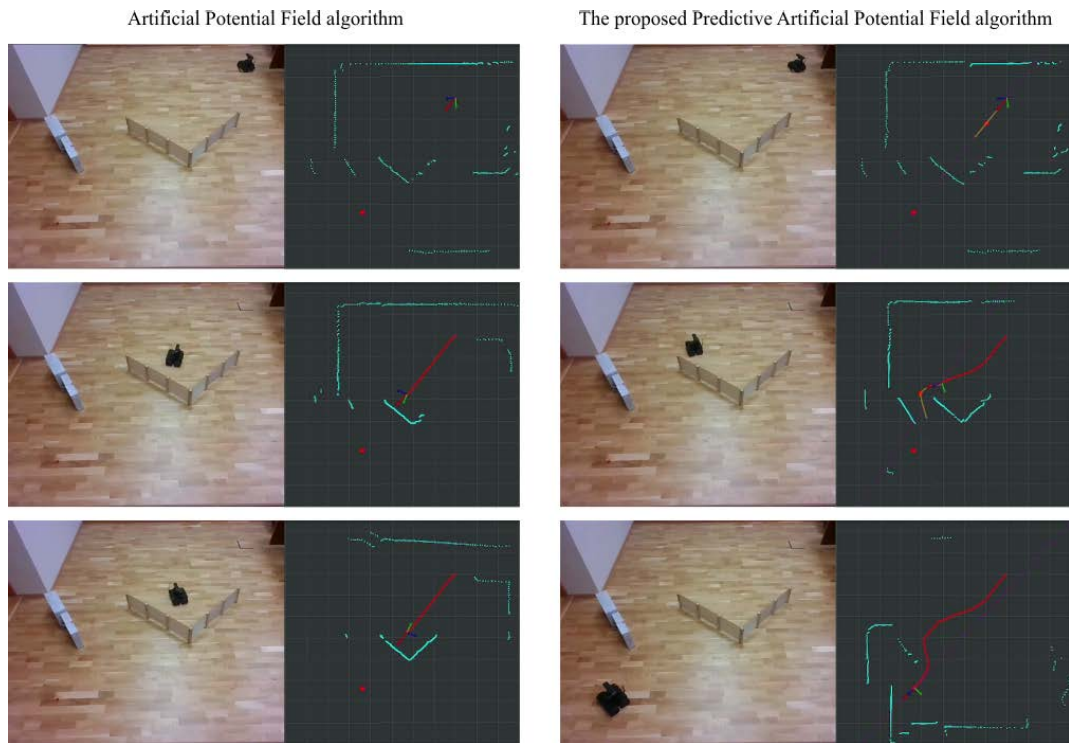


FIGURE 12. Comparison of the proposed PAPF and the classical APF algorithms in Test (V).

One can see, that calculation time depends linearly on step-size and horizon of prediction. The path planning algorithm control loop period was set to 100 ms. For this reason, the authors decided to chose step-size equal to $\Delta = 0.03$.

Such a step-size does not impact significantly on the quality of predicted path, but significantly reduce the calculation time. It has been assumed that additional 25% of horizon of prediction ($\lambda_{stagnation} = 25\% \cdot \lambda$) is calculated for detection

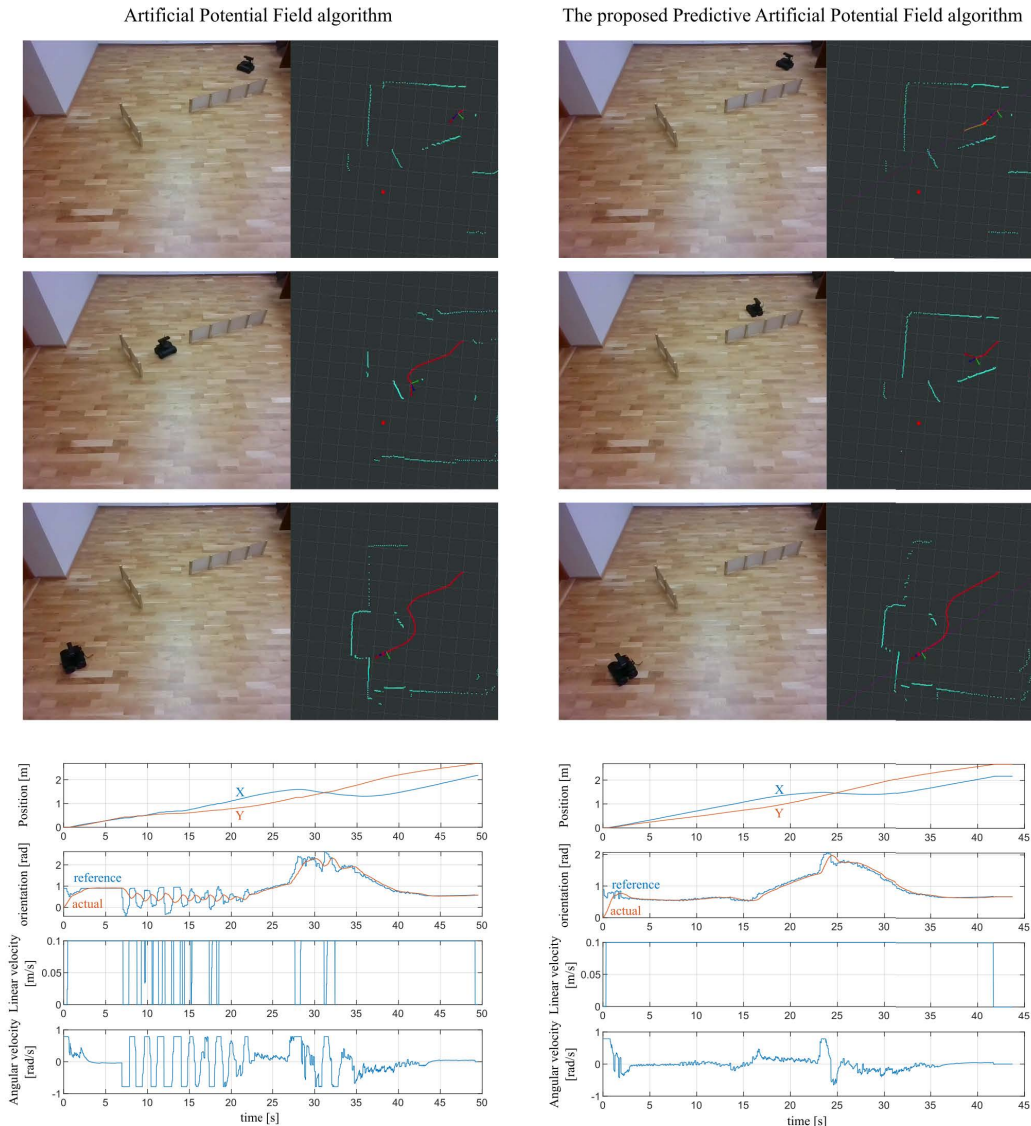


FIGURE 13. Comparison of the proposed PAPF and the classical APF algorithms in Test (VI) with additional subplots presenting position, orientation, linear velocity and angular velocity in time domain.

of stagnation. In a case of obstacle-free environment, the AGV covers a distance equal to $\lambda_{stagnation}$, while in the case of local minimum presence, the AGV stagnates and the distance is shorter. The stagnation occurs if the distance covered by AGV is less than a half of the distance which should travel in straight line. Due to this, the radius R was set to 25% $\lambda_{stagnation}$.

The proposed PAPF has been evaluated considering the following aspects:

- impact of the horizon of prediction parameter to AGV behaviour and traveled path,
- comparison of original APF and the proposed PAPF taking into account the time required for goal reaching, and the traveled path length,
- energetic efficiency of the proposed PAPF in comparison to the original PAPF.

A. HORIZON OF PREDICTION

As was mentioned in Section III, the horizon of prediction value should be selected considering the AGV, environment, and assumed obstacles dimensions, but also the used sensor and AGV's perception, due to the proposed PAPF is still a local path planning algorithm. Another aspect is related to computational requirements, i.e. performance of AGV computer, control loop period and expected number of predicted points. The longer path is predicted in the PAPF, then the AGV will react in advance to obstacle, but if the predicted path will be too long, then the prediction may be generated without information about the environment behind the obstacle, and may provide imprecise prediction of future movements in complex environment. In Fig. 7, the traveled paths of the original APF and the proposed PAPF for 5 different horizon of prediction ($\lambda \in \{0.5, 0.75, 1.0, 1.5, 2.0\}$ m)

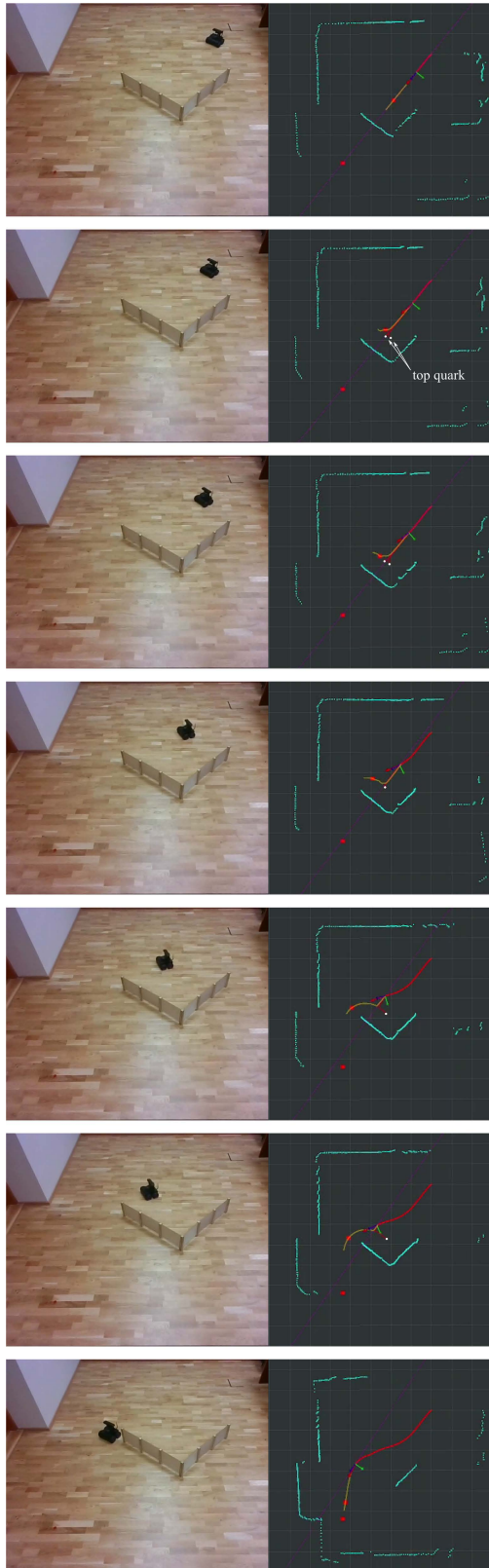


FIGURE 14. Local minimum avoidance using the proposed PAFP algorithm.

are presented. The obtained results in form of videos are also attached as supplementary file. The AGV goal position

was a 7 m from a robot in the straight path. One can see that longer horizon of prediction provides the smoother and shorter path. For horizon of prediction equal to 2 m, an unsmooth movement occurs (orange rectangle in Fig. 7), which was caused by above-mentioned inaccurate prediction in long horizon due to lack of perception behind the obstacle. Analysing size of the Husarion ROSbot 2.0 PRO and the available environment, the Authors selected horizon of prediction equal to 1 m for next examinations. This value of λ provides significantly smoother and shorter path.

B. EXAMINATIONS

Both algorithms have been evaluated in six environments. The environments have been created to present behaviour of APF and the proposed PAFP in narrow passages, driving along the long wall and in occurrence of local minimum. Another aspect was to create an environments where there is an obstacle between the AGV and the temporary goal to validate the collision-free operation of the proposed approach.

The obtained results are presented in the form of three selected moments in Fig. 8-13 for Test (I)-(VI), respectively. These are also attached as videos in supplementary file. In figures at left column an original APF is presented, while at right column is the proposed PAFP. Each captured moment of experiment consists of two elements: the real photo and the current perception of the robot visualized in RViz package (the part of the ROS). The RViz presents, the AGV's position and orientation, calculated output direction by path planning algorithm, and marked as red line, already traveled path. In a case of the proposed PAFP, there is additional drawings: (i) orange line is a predicted path, (ii) red point at the predicted path is a temporary goal, and (iii) in a case of local minimum within a horizon of prediction, a light red path as abandoned predicted path with placed a *top quark* at the stagnation point marked as white dot. In Fig. 13, the additional plots of mobile robot's position, orientation, and linear and angular velocities in time domain have been presented under the captured moments of experiments. Additional captured moments related to local minimum avoidance are presented in Fig. 14. The path's quality indicators, i.e., duration of the movement and path length, are summarized in Table 2.

One can see that the proposed PAFP provides much smoother path. The predicted trajectory successfully gives the information about the new temporary point, and the goal position is reached faster than the original APF. From the plots presented in Fig. 13, one can see that the robot oscillations occur for original APF due to limited dynamic of the mobile robot, i.e. reference signal is changing faster than mobile robot can reach it. In such a case, the linear velocity is reduced for APF algorithm due to eq. 5. In the proposed PAFP, the reference orientation is much smoother, and there is no reason to reduce the linear velocity. The indicators presented in Table 2 proves the efficiency of the proposed PAFP. The time required to reach the goal is around 21.5 % shorter than the original APF, and also the traveled path is significantly shorter by up to 8.29 %.

In Test (III), the proposed PAPF presents that even in narrow gap, the algorithm provides collision-free path, and still the traveled path in comparison to original APF in that part of environment is much smoother.

C. ENERGETIC EFFICIENCY MEASUREMENT

As was mentioned in Section II, the smoother path, shorter path, and less time required to reach the goal should provide significant improvement of energetic efficiency. To prove that assumption, the energy consumption of ROSbot 2.0 PRO with the original APF and with the proposed PAPF path planners have been compared. The efficiency measurement were performed using the XTAR VC4S battery charger. The batteries used in the mobile robot are 3x XTAR 18650-350PCM 3500mAh Li-ION Protected 3,7V 10A. The procedure of the measurement was as follows:

- charge the batteries,
- program the robot to start experiment automatically,
- insert fully charged batteries,
- turn on the mobile robot,
- turn off the mobile robot right after the goal is reached,
- charge the batteries and sum the read the charged capacities.

To provide higher accuracy of efficiency measurements, each experiment was performed 3 times, i.e. 3 experiments for original APF, and 3 experiment for the proposed PAPF. The goal was $\langle 10, 0 \rangle$ m and three obstacles were placed in the AGV's path, similar to setup presented in Fig. 7. The obtained results are as follows:

- original APF: 149.7 mAh
- the proposed PAPF: 117.6 mAh

The application of the proposed PAPF allowed to reduce electric energy consumption by 32.1 mAh (21.4 %).

V. CONCLUSION

Application of the proposed algorithm into the local path planning algorithm results in a significant reduction of consumed energy, goal reaching time, and path length. The original APF algorithm has been used in both: the prediction of future movement of the AGV, and as local path planning algorithm with a new temporary goal instead of the global one. Such a combination guarantees the collision-free operation, smoother movement and shorter path selection. The proposed approach allows to decrease power consumption by over 20%.

Moreover, the proposed algorithm allows to bypass the local minimum. The proposed *top quark*-based mechanism prevents the AGV from stagnation in a local minimum, and allows to bypass the local minimum with a smooth movement. The results are also presented in video form included as supplementary files. The proposed local path planning algorithm should be considered in industrial AGVs, where the energy-efficiency is very important due to significant payload. In case of transportation of pallets with weight up to 300 kg, the non-smooth movement provided by the

original APF algorithm would significantly decrease the current batteries capacity. It has been experimentally proved that the proposed approach successfully solves the problem of non-smooth movement. Another aspect important for the application is time required to reach the goal. The proposed approach significantly decreases the task execution time.

Future work will focus on dynamic obstacles avoidance in an energy-efficient way. The research group's aim of research related to local path planning algorithms is to provide the efficient algorithm that can be safely implemented in industrial AGVs in dynamic environments and with significant payload. In such a case, the smoothness of the robot's path and its continuous movement have a significant impact to energetic-efficiency and production rate due to availability to execute more tasks per single batteries charge.

APPENDIX

The brief presentation of the proposed Predictive Artificial Potential Field algorithm one can see in the following URL:

<https://youtu.be/FJSIUPzLjqQ>

or QR code:



REFERENCES

- [1] F. Gul, I. Mir, L. Abualigah, P. Sumari, and A. Forestiero, "A consolidated review of path planning and optimization techniques: Technical perspectives and future directions," *Electronics*, vol. 10, no. 18, p. 2250, Sep. 2021.
- [2] M. Hirata, M. Tsukada, K. Okumura, Y. Tamura, H. Ochiai, and X. Defago, "Roadside-assisted cooperative planning using future path sharing for autonomous driving," in *Proc. IEEE 94th Veh. Technol. Conf. (VTC-Fall)*, Sep. 2021, pp. 1–7.
- [3] T. Shimmura, R. Ichikari, T. Okuma, H. Ito, K. Okada, and T. Nonaka, "Service robot introduction to a restaurant enhances both labor productivity and service quality," *Proc. CIRP*, vol. 88, pp. 589–594, Jan. 2020.
- [4] K. H. Seo and J. H. Lee, "The emergence of service robots at restaurants: Integrating trust, perceived risk, and satisfaction," *Sustainability*, vol. 13, no. 8, p. 4431, Apr. 2021.
- [5] M. N. Zafar and J. C. Mohanta, "Methodology for path planning and optimization of mobile robots: A review," *Proc. Comput. Sci.*, vol. 133, pp. 141–152, Jan. 2018.
- [6] R. Szczepanski and T. Tarczewski, "Global path planning for mobile robot based on artificial bee colony and Dijkstra's algorithms," in *Proc. IEEE 19th Int. Power Electron. Motion Control Conf. (PEMC)*, Apr. 2021, pp. 724–730.
- [7] S. Zaman, W. Slany, and G. Steinbauer, "ROS-based mapping, localization and autonomous navigation using a pioneer 3-DX robot and their relevant issues," in *Proc. Saudi Int. Electron., Commun. Photon. Conf. (SIECPC)*, Apr. 2011, pp. 1–5.

- [8] A. Gasparetto, P. Boscariol, A. Lanzutti, and R. Vidoni, "Path planning and trajectory planning algorithms: A general overview," in *Motion and Operation Planning of Robotic Systems*. Cham, Switzerland: Springer, 2015, pp. 3–27.
- [9] F. Gul, W. Rahiman, and S. S. N. Alhady, "A comprehensive study for robot navigation techniques," *Cogent Eng.*, vol. 6, no. 1, Jan. 2019, Art. no. 1632046.
- [10] H. Li, Y. Luo, and J. Wu, "Collision-free path planning for intelligent vehicles based on Bézier curve," *IEEE Access*, vol. 7, pp. 123334–123340, 2019.
- [11] E. W. Dijkstra, "A note on two problems in connexion with graphs," *Numer. Math.*, vol. 1, no. 1, pp. 269–271, Dec. 1959.
- [12] M. Luo, X. Hou, and J. Yang, "Surface optimal path planning using an extended Dijkstra algorithm," *IEEE Access*, vol. 8, pp. 147827–147838, 2020.
- [13] F. Peralta, M. Arzamendia, D. Gregor, D. G. Reina, and S. Toral, "A comparison of local path planning techniques of autonomous surface vehicles for monitoring applications: The Ypacarai lake case-study," *Sensors*, vol. 20, no. 5, p. 1488, Mar. 2020.
- [14] A. A. Ravankar, A. Ravankar, T. Emaru, and Y. Kobayashi, "HPPRM: Hybrid potential based probabilistic roadmap algorithm for improved dynamic path planning of mobile robots," *IEEE Access*, vol. 8, pp. 221743–221766, 2020.
- [15] H. J. Zhang, "Path planning of industrial robot based on improved RRT algorithm in complex environments," *IEEE Access*, vol. 6, pp. 53296–53306, 2018.
- [16] U. Orozco-Rosas, K. Picos, and O. Montiel, "Acceleration of path planning computation based on evolutionary artificial potential field for non-static environments," in *Intuitionistic and Type-2 Fuzzy Logic Enhancements in Neural and Optimization Algorithms: Theory and Applications*. Cham, Switzerland: Springer, 2020, pp. 271–297.
- [17] U. Orozco-Rosas, O. Montiel, and R. Sepúlveda, "Mobile robot path planning using membrane evolutionary artificial potential field," *Appl. Soft Comput. J.*, vol. 77, pp. 236–251, Apr. 2019.
- [18] M. D. Phung and Q. P. Ha, "Safety-enhanced UAV path planning with spherical vector-based particle swarm optimization," *Appl. Soft Comput.*, vol. 107, Aug. 2021, Art. no. 107376.
- [19] X.-H. Liu, D. Zhang, J. Zhang, T. Zhang, and H. Zhu, "A path planning method based on the particle swarm optimization trained fuzzy neural network algorithm," *Cluster Comput.*, vol. 24, no. 3, pp. 1901–1915, Sep. 2021.
- [20] X. Zhou, F. Gao, X. Fang, and Z. Lan, "Improved bat algorithm for UAV path planning in three-dimensional space," *IEEE Access*, vol. 9, pp. 20100–20116, 2021.
- [21] C. Miao, G. Chen, C. Yan, and Y. Wu, "Path planning optimization of indoor mobile robot based on adaptive ant colony algorithm," *Comput. Ind. Eng.*, vol. 156, Jun. 2021, Art. no. 107230.
- [22] F. Gul, W. Rahiman, S. S. N. Alhady, A. Ali, I. Mir, and A. Jalil, "Meta-heuristic approach for solving multi-objective path planning for autonomous guided robot using PSO–GWO optimization algorithm with evolutionary programming," *J. Ambient Intell. Hum. Comput.*, vol. 12, no. 7, pp. 7873–7890, Jul. 2021.
- [23] O. Khatib, "Real-time obstacle avoidance for manipulators and mobile robots," in *Proc. IEEE Int. Conf. Robot. Autom.*, Mar. 1985, pp. 500–505.
- [24] H. Sang, Y. You, X. Sun, Y. Zhou, and F. Liu, "The hybrid path planning algorithm based on improved A* and artificial potential field for unmanned surface vehicle formations," *Ocean Eng.*, vol. 223, Mar. 2021, Art. no. 108709.
- [25] Y. Koren and J. Borenstein, "Potential field methods and their inherent limitations for mobile robot navigation," in *Proc. IEEE Int. Conf. Robot. Automat.*, vol. 2, Apr. 1991, pp. 1398–1404.
- [26] P. Lin and M. Tsukada, "Model predictive path-planning controller with potential function for emergency collision avoidance on highway driving," *IEEE Robot. Autom. Lett.*, vol. 7, no. 2, pp. 4662–4669, Apr. 2022.
- [27] R. Szczepanski, A. Bereit, and T. Tarczewski, "Efficient local path planning algorithm using artificial potential field supported by augmented reality," *Energies*, vol. 14, no. 20, p. 6642, Oct. 2021.
- [28] J. Batista, D. Souza, J. Silva, K. Ramos, J. Costa, L. dos Reis, and A. Braga, "Trajectory planning using artificial potential fields with metaheuristics," *IEEE Latin Amer. Trans.*, vol. 18, no. 5, pp. 914–922, May 2020.
- [29] P. Lin, W. Y. Choi, and C. C. Chung, "Local path planning using artificial potential field for waypoint tracking with collision avoidance," in *Proc. IEEE 23rd Int. Conf. Intell. Transp. Syst. (ITSC)*, Sep. 2020, pp. 1–7.
- [30] U. Orozco-Rosas, K. Picos, and O. Montiel, "Hybrid path planning algorithm based on membrane pseudo-bacterial potential field for autonomous mobile robots," *IEEE Access*, vol. 7, pp. 156787–156803, 2019.
- [31] Y. Du, X. Zhang, and Z. Nie, "A real-time collision avoidance strategy in dynamic airspace based on dynamic artificial potential field algorithm," *IEEE Access*, vol. 7, pp. 169469–169479, 2019.
- [32] Q. Yao, Z. Zheng, L. Qi, H. Yuan, X. Guo, M. Zhao, Z. Liu, and T. Yang, "Path planning method with improved artificial potential field—A reinforcement learning perspective," *IEEE Access*, vol. 8, pp. 135513–135523, 2020.
- [33] P. Lin, W. Y. Choi, S.-H. Lee, and C. C. Chung, "Model predictive path planning based on artificial potential field and its application to autonomous lane change," in *Proc. 20th Int. Conf. Control, Autom. Syst. (ICCAS)*, Oct. 2020, pp. 731–736.
- [34] J. Song, C. Hao, and J. Su, "Path planning for unmanned surface vehicle based on predictive artificial potential field," *Int. J. Adv. Robotic Syst.*, vol. 17, no. 2, Apr. 2020, Art. no. 1729881420918461.
- [35] K. Wyrąbkiewicz, T. Tarczewski, and Ł. Niewiara, "Local path planning for autonomous mobile robot based on apf-bug algorithm with ground quality indicator," in *Advanced, Contemporary Control*. Cham, Switzerland: Springer, 2020, pp. 979–990.
- [36] S. Liu and D. Sun, "Modeling and experimental study for minimization of energy consumption of a mobile robot," in *Proc. IEEE/ASME Int. Conf. Adv. Intell. Mechatronics (AIM)*, Jul. 2012, pp. 708–713.



RAFAL SZCZEPANSKI (Member, IEEE) received the B.Sc. degree in automatics and robotics and the M.Sc. degree in informatics from Nicolaus Copernicus University in Torun, in 2016 and 2017, respectively. He is currently pursuing the Ph.D. degree in automatics and robotics with the Warsaw University of Technology. He is also employed as an Assistant at the Department of Automatics and Measurement Systems, Nicolaus Copernicus University in Torun. His research interests include adaptive control of electrical drives, nature-inspired optimization algorithms, and path planning algorithms for mobile robots.



TOMASZ TARCZEWSKI (Member, IEEE) received the M.Sc. degree in automatics and robotics from the Poznan University of Technology, in 2005, and the Ph.D. and D.Sc. degrees in automatics and robotics from the Warsaw University of Technology, in 2010 and 2019, respectively. Since 2010, he has been with Nicolaus Copernicus University in Torun, where he is currently employed as an Associate Professor at the Department of Automatics and Measurement Systems. His research interests include automatic control in drives and mobile robots, with emphasis on optimal, predictive, and adaptive control algorithms for these systems, as well as nature-inspired optimization methods.



KRYSTIAN ERWINSKI (Member, IEEE) received the M.Sc. degree in technical physics from Nicolaus Copernicus University in Torun, in 2008, and the Ph.D. degree in automatics and robotics from the Warsaw University of Technology, in 2014. He is currently employed as an Assistant Professor at the Department of Automatics and Measurement Systems, Nicolaus Copernicus University in Torun. His research interests include trajectory and velocity profile optimization, nature-inspired optimization algorithms, and industrial communication.

...